Silicon Nanomembranes for Efficient and Precise Molecular Separations

Karl J. P. Smith,[1] Joshua D. Winans,[2] James L. McGrath[2*]

[1]Department of Biochemistry and Biophysics, University of Rochester School of Medicine,
[2]Department of Biomedical Engineering, University of Rochester

[*]To whom correspondence should be addressed; E-mail: jmcgrath@bme.rochester.edu

Nanoporous silicon membranes are capable of making molecularly thin sieves, which are useful for macromolecule separations. Here we discuss what makes the thinness of silicon nanomembranes important for sieving, the various techniques being explored to patterning pores into them, and the areas where these membranes could see immediate application.

Introduction

The need to separate similarly sized molecules in solvent is a ubiquitous problem in modern medical, pharmaceutical, and industrial processes. Membranes that can act as sieves and hold back larger molecules while allowing smaller molecules to pass have been used in laboratory preparations of proteins since the 1920s [1], for blood dialysis since the 1940s [2] and have been used for solute recovery in industrial processes beginning in the 1960s [3]. Today membrane technology is its own industry. 250 million ultrafiltration membranes for dialysis were sold worldwide in 2013, with dialysis products representing

more than 14.2 billion dollars in sales that year [4]. Membranes used for biotechnology products represented sales of 80 million dollars in 2010 in the United States alone, with sales expected to reach 130 million in 2015 [5].

Macromolecule separations fall in the category of ultrafiltration, which by definition uses membranes with pore sizes in the range of ∼5 - 100 nm. Membranes with smaller pores, such as those used for reverse osmosis processes, are considered nanofiltration membranes, while membranes with larger pores are considered microfilters. Both nano- and microfilters are outside the scope of this work.

1 Separation Science

The flux of solute molecules (N) through a membrane can be understood as the sum of the diffusive and convective contributions to flux:

$$\text{Solute Flux} = N = -K^{-1} D_\infty \frac{dC}{dz} + GVC \tag{1}$$

where D_∞ is the diffusivity of a solute molecule as given by the Stokes-Einstein equation, C is concentration, z is distance from the pore, and K^{-1} and G represent diffusive and convective hindrance factors, respectively, which are related to the hydrodynamic drag. The hindrance factors are non-trivial to calculate (although as early as 1936 Ferry had derived values based on steric considerations [6]) and the primitive state of membrane technology before the 1970s meant that theoretical predictions were difficult to experimentally verify. With the invention of track-etched membranes (see section 2.2), which have nearly cylindrical pores that are fairly uniform, there was a flurry of experimental and theoretical activity culminating in Deen's 1987 review [7], which put the calculation of hindrance factors for dilute uncharged spherical molecules moving through uniform cylindrical or slit pores on firm analytical ground. This work has since been extended to cover

charge-charge interactions between the molecule and the pore [8, 9, 10], non-spherical molecules [11], non-uniform pore distributions [12] and various speeds of filtration [13].

Because silicon nanomembranes are typically at least an order of magnitude thinner than other ultrafiltration membranes, diffusion continues to be a relevant process over the course of an experiment [13]. The Péclet number Pe is the ratio of convective to diffusive flux through a membrane and is given by Equation 2.

$$Pe = \frac{WVL}{HD_\infty} \tag{2}$$

where V is the particle velocity and L is the thickness of the membrane, and H and W are the radially averaged versions of the hindrance factors K^{-1} and G, respectively, in Equation 1. If the Pe of a system is greater than 1, convection dominates the behavior of the separation, while a $Pe > 1$ corresponds to a diffusion-dominated separation. Assuming we have a monomeric protein with a hydrodynamic radius of 4 nm, such as BSA ($D_\infty \approx 1 \times 10^{-6}\text{cm}^2/\text{s}$), 40 nm effective diameter pores in our membrane, and a transmembrane velocity of 0.1 cm/s, we can estimate $W = 0.9$ and $H = 0.6$ [14]. A 1 μm polymeric membrane would have a Pe of ~ 15, while a 50 nm silicon nano membrane would have a Pe of 0.75, meaning that by nature of their thinness silicon nitride membranes are in a filtration regime not accessible to thicker membranes, which can lead to improved performance [13].

Most practical separations cannot occur at nearly infinite dilutions. As molecules are hindered with respect to solvent velocity, they accumulate at the membrane, leading to concentration increases at the membrane surface on the order of 20 to 50 times that in bulk solution [1]. This concentration polarization leads to increased hydraulic resistance, and as the protein layer acts as a second membrane it can dramatically change the hindrance factors and separation characteristics of the membranes [15, 16]. If left unchecked, the

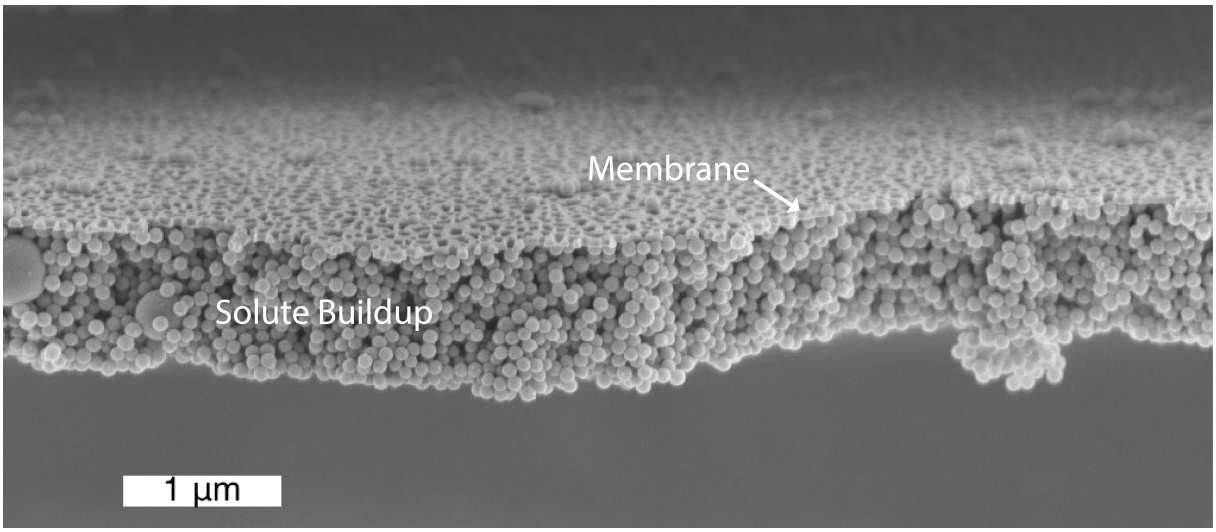

Figure 1: 100 nm polystyrene nanoparticles move slower than the water they are suspended in (in this separation they are totally retained by the membrane), and build up behind an NPN silicon nitride membrane (section 2.1), creating an extended region of hydraulic resistance. The flow in this separation was from the bottom of the image towards the top

buildup forms an irreversible cake layer on the surface [17], although this cake layer is dependent on the surface chemistry of the membrane. Stirred cells and tangential flow setups are used to ameliorate this buildup, but even with these technologies a stagnant layer of increased solute concentration builds up against the membrane [18] (Figure 1). If the separation occurs without a transmembrane pressure drop (as in dialysis), the opposite problem can occur, where solute flux across the membrane leads to a depletion layer above the membrane. Again, stirred cells and tangential flow setups are used to minimize this.

The majority of membranes used in medicine, industry, and biopharmaceutical separations are not track-etched membranes, and instead are formed of cross-linked polymer fibers (Figure 2), meaning that molecules and solvent must take long and tortuous routes to get through the membrane. This decreases the permeability of the membrane, results in broad (log-normal) pore size distributions [19], and dramatically increases the available

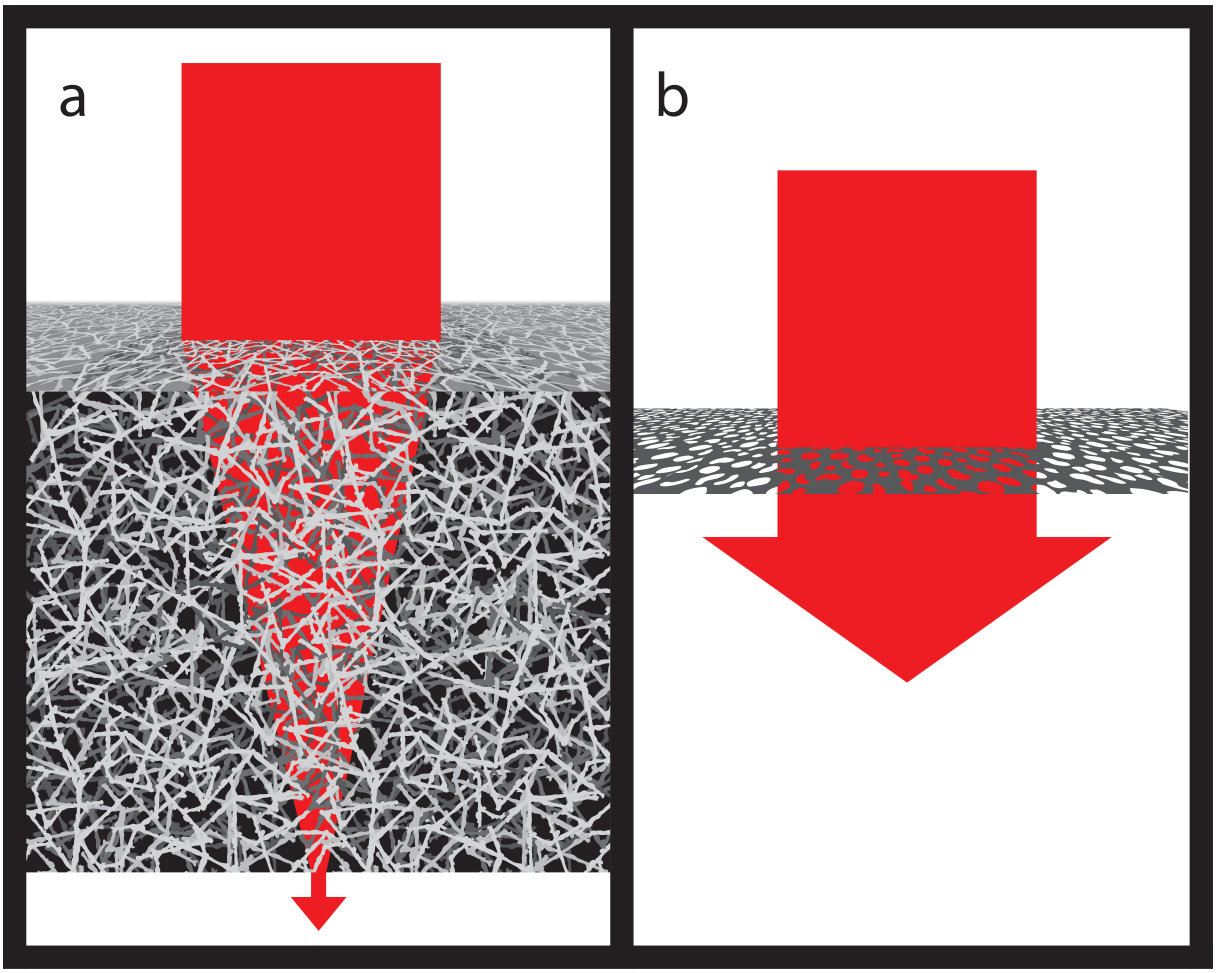

Figure 2: Reconstituted Cellulose membranes (a) are composed of interlocking fibers, and are quite thick. Water and particles must take tortuous paths through it, decreasing flux. Flux through a silicon nanomembrane (b), by contrast, moves directly through short channels, leading to higher hydraulic permeabilities.

surface area that solutes can bind to (which both wastes precious solute and contributes to fouling). These downsides to polymeric membranes are accepted by end users because such membranes are cheap, robust, and easily tailored to particular separations. Hydrophilic membranes, such as those made out of cellulose, also are highly resistant to irreversible fouling without chemical treatment of their surface [20]. Detailed comparisons of many commercially available cross-linked polymer membranes by Mehta et. Al. [21]) reveal that there is an inherent trade-off between selectivity and permeability - as effective pore size gets smaller, more of a macromolecule of interest can be held back behind a membrane and concentrated, but smaller pores mean hydraulic permeability decreases and separation processes either require more pressure to drive them or take longer to happen. In fact, this trade-off, demonstrated in Figure 3, gives rise to a characteristic curve. One way to improve upon the performance of these membranes and beat the curve of death is to use membranes with cylindrical or slit-shaped pores. Flow through such cylindrical pores is governed by the familiar Hagen-Pouiselle equation when these pores are of infinite length. Dagan extended this using a computational approach to very thin membranes, where pore length approaches the pore diameter (Equation 3)

$$Q = \frac{\Delta P r^3}{\mu \left[3 + \frac{8}{\pi}\left(\frac{l}{r}\right)\right]} \tag{3}$$

where Q, μ, r, and l are the solvent flux, solvent viscosity, pore radius, and pore length, respectively. (Sampson, in 1891, derived analytically the limiting case of infinitely thin pores [23]). Tortuous path membranes have complex geometry, and never develop the characteristic parabolic flow trajectory of the cylindrical pores, which leads to lower solvent flux. A further way to decrease hydraulic resistance without changing separation characteristics is to use thinner membranes. Although the Dagan equation predicts only a linear relationship between volumetric flow rate and pore length, because commercial

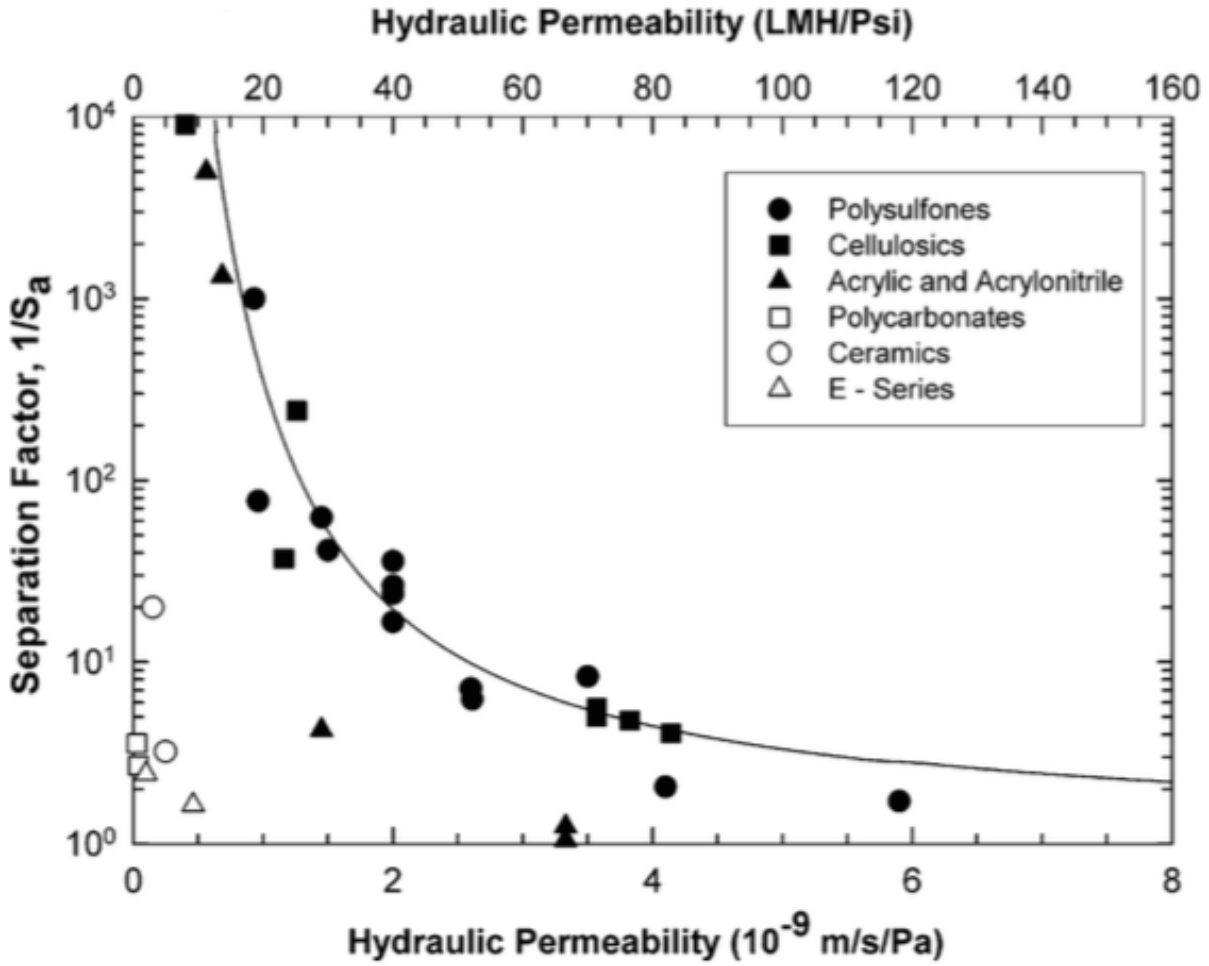

Figure 3: Selectivity-permeability trade-off for a set of commercial ultrafiltration membranes using Bovine Serum Albumin (BSA) as a model protein. Separation factor refers to the relative amounts of BSA before and after the membrane, with a separation factor of 0 corresponding to no membrane at all. Note that hydraulic permeabilities of up to 67×10^{-9} m/s/Pa have been reported for silicon nanomembranes [22]. Solid curve represents a model calculation. Image taken from [21].

membranes are at least an order of magnitude thicker than silicon nanomembrane (pnc-Si nanomembranes as thin as 15 nm have been used for separations [24]), that corresponds to an order of magnitude increase in hydraulic permeability (see Figure 3). Similarly, an increase in the number of pores (an increase in porosity) would also increase the hydraulic permeability, and as long as the new pores did not change the pore size distribution, the separation characteristics should not change.

Selectivity can also be improved without sacrificing permeability by increasing the uniformity of pores in the membrane. Because of the r^4 dependence on flux through a cylinder (Equation 3), the larger pores in a distribution of sizes dominate the hydraulic flux. The larger pores also define the separation characteristics, since the molecules that are rejected by the largest pore in the membrane will likewise be rejected by the entire membrane, but molecules of a size that gets rejected by the smallest pores very well might pass through larger pores. For this reason, a highly porous (a high porosity) membrane with a wide distribution of pore sizes is very nearly equivalent to a very low porosity membrane composed of only the largest pore sizes in the distribution - the smaller pores may as well be closed. In the case where large pores are not numerous enough to dominate flux behavior, very tight molecular weight cutoffs still cannot be achieved, since some higher weight species will make it through the large pores.

In summary, current commercial membranes have a clearly defined permeability-selectivity tradeoff. To improve performance, next generation membranes will need to be thinner, more porous, have simple pore geometries such as slits or cylinders, and have tight pore size distributions. Charging membranes with surface chemistries designed to repel target molecules has also been pursued as a way to increase selectivity without decreasing permeability [21], but is outside the scope of this work.

Recent advancements in making anodized aluminum [25, 26], Carbon nanotube [27,

28, 29], and block copolymer [30] membranes have shown promise, but these technologies tend to lead to thick membranes that are brittle and difficult to manufacture in a scalable way.

2 Silicon Nanomembranes

Perhaps the most obvious approach to create next generation filters is to build upon the extraordinary advances made in silicon wafer technology as part of the semiconductor industry over the past 60 years. Silicon fabrication is a mature technology, and porous freestanding membranes with thicknesses in the tens of nanometers made out of silicon dioxide, nanocrystalline silicon, and silicon nitride have proven mechanically robust enough to be used for separations. Silicon substrates are generally much more biocompatible than traditional cellulose membranes, with early reports characterizing the material as intrinsically anti-fouling by comparison [31]. Silicon and polysilicon both have levels of coagulation and complement activation comparable to Teflon and stainless steel (both of which are already ubiquitous in medical implants). However, unmodified silicon has significantly higher platelet activation as compared to Teflon [32] and is more prone to having proteins foul or stick to the surface. For this reason, Polyethylene glycol (PEG) is covalently bonded to nanoporous silicon substrates used for ultrafiltration [33, 34, 35]. As a hydrophilic polymer, PEG-lyated silicon surfaces are less prone to protein fouling [33] and have platelet activation comparable to Teflon. The coating is also quite stable, protecting surfaces for up to four weeks in *in vivo*-like conditions [36]. Additionally, human renal proximal tubule cells have been grown and shown to function on a PEG-lyated silicon surface, which further indicates the membranes are not cytotoxic [37]. Aminosilanization is also sometimes performed on silicon nanomembranes, either as a precursor to PEG-lyation or to impart a positive charge on the filter surface [38, 39].

Patterning or growing pores in the membrane has proven to be the most difficult step. The first attempts used standard lithography approaches to pattern holes directly into a silicon substrate. The inherent limitations of this technology (feature sizes - such as pores - must be larger than half the wavelength of the light used) meant that the minimum pore size achievable through this method is $\sim$0.5 μm - too large for most macromolecule separations. Since that time, a variety of other approaches to pattern (or grow, in the case of pnc-Si) pores in thin film silicon-based substrates have been demonstrated, which are detailed below.

2.1 Porous Nanocrystalline Silicon

Discovered serendipitously in 2007 [24], porous nanocrstalline silicon (pnc-Si) is generated using a thin (15 nm - 50 nm) film of amorphous silicon sandwiched between two oxide layers. When the stack is rapidly heated, an incompletely understood interfacial interaction causes voids to form in the amorphous layer. If the sandwiching oxide layers are etched away, the voids become pores in a thin freestanding membrane. The pore formation process can generate different pore size distributions and porosities by changing the heating conditions or the thickness of the amorphous oxide layer, with final average pore sizes tunable within the range of 5-50 nm. Pore size distributions are tight compared to commercial membranes, with the largest pores in the membrane typically twice as large as the average pore size, and typical porosities are between 5 and 20% of total membrane area. The membranes demonstrate remarkably high hydraulic permeabilities, of up to 67 m/s/Pa, which is higher than any other existing nanoporous membrane [22], and extremely tight cutoffs (less than 10 nm) during pressurized protein [40] and gold nanoparticle separations [22]. Further, the extreme thinness of the membrane means that the membrane has essentially no resistance to the diffusion of small molecules at sizes of

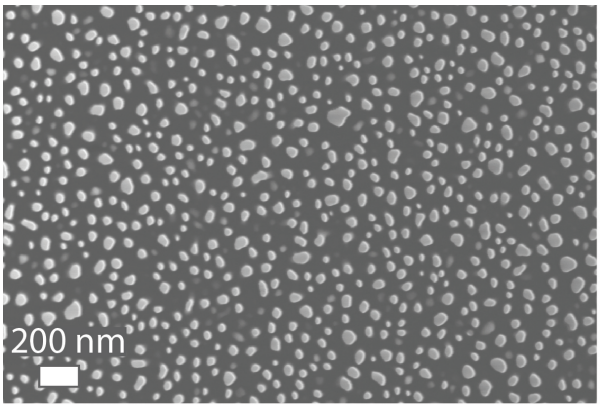

NPN using pnc-Si as a template.

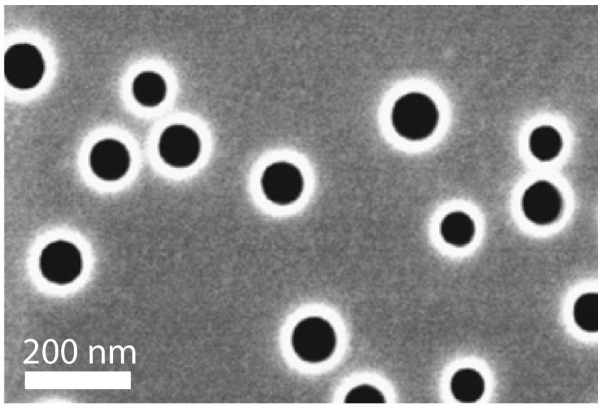

Track etched Silicon Nitride.
Taken from Zhang et. Al.

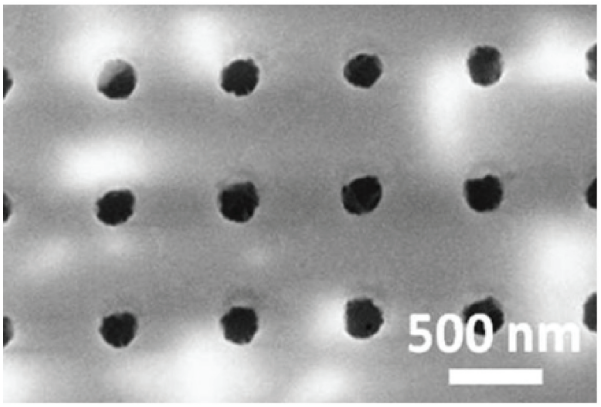

Interferometric. Taken from Ileri et. Al.

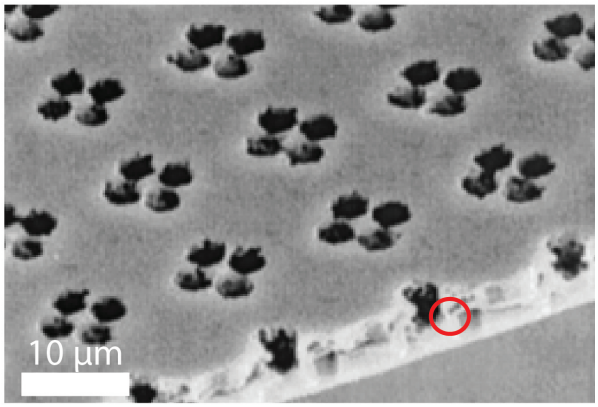

Micromachined. Red circle indicates
actual restricting pore. Desai et. Al.

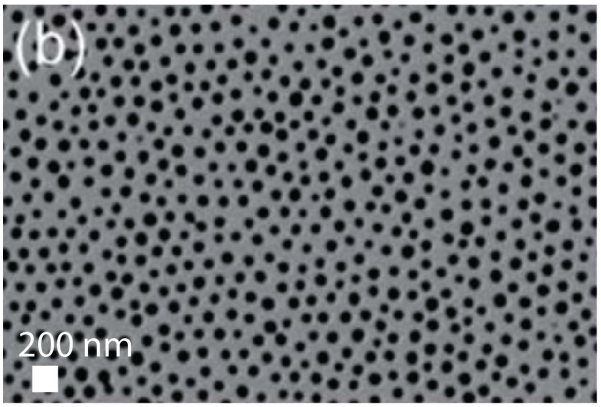

Block copolymer templated.
From Montagne et. Al.

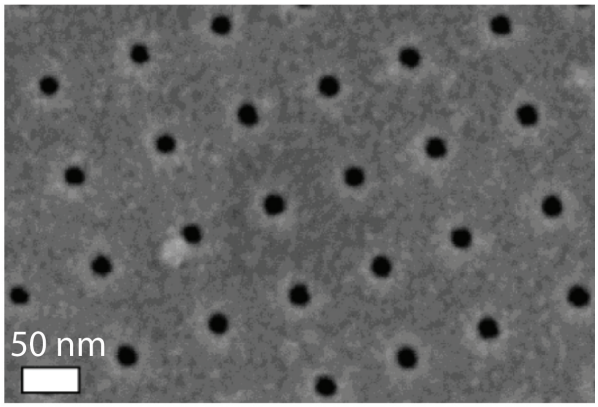

FIB drilled nanopores in Silicon Nitride.
From Tong et. Al.

10% of the pore size [41]. While a substantial amount of separations data was collected using pnc-Si, the low intrinsic strength of the crystallized silicon meant the membranes were prone to breaking, leading to low yields and requiring great care in the handling of the chips. For this reason, pnc-Si has since been used as a template for transferring pore distributions onto a thin film of Nanoporous Silicon Nitride (NPN) using reactive ion etching. As a result of the pore transfer process, NPN membranes can have higher porosities (up to 40%) and larger average pore sizes (40-80 nm), but are still stronger. The tightness of the pore size distribution is maintained in the new material, and in nanoparticle separations they demonstrate the same remarkable size cutoffs in separations ($\sim$10 nm) [42].

2.2 Track-etched

The original track etch process uses a cyclotron to generate heavy ion radiation, which is used to bombard a polycarbonate substrate. As the heavy ions pass through the plastic, they leave 'tracks' which are afterwards chemically etched to form very uniform and cylindrical pores. The resultant membranes, though thinner than cellulose membranes, are still quite thick (6-10 μm) [43], and beginning in 2008 SiN films have been used as an alternate substrate for track-etching [44]. As in standard track-etching processes, the pores are either conical or double-conical with fairly broad distributions (standard deviations of $\sim$20%) with the distribution tunable by etching times and the heavy ion flux. The strength of the silicon substrate allows relatively thin membranes ($\sim$100 nm), but the process has hard upper bounds on porosity, as the stochastic nature of the irradiation means pores begin to overlap when porosities exceed 2% [33]. The manufacture of these membranes also requires access to a cyclotron.

2.3 Inferometric

Traditional lithography techniques depend on masks, which have a spatial resolution of ~ 0.5 μm because of the UV light dispersion around the holes in the photo mask. Smaller features are possible but require dedicated setups and are uneconomical [45]. Laser Interferometric Lithograph (LIL) is a maskless process that uses the standing waves of the interference of two or more lasers to produce activated patterns in a photoresist, which are then chemically etched to reveal circular, or even pyramidal pores [46]. The pores are periodic and monodisperse (variation of about 25%), with porosities of about 19% and a final thickness of 220 nm, and the process is easy to scale up [43]. Typical average pore sizes are between 150 - 250 nm, meaning the membranes so far are only useful for the extreme upper edge of ultrafiltration, although they have already proven useful in microfiltration [45].

2.4 Micromachined

Membranes of this type use the growth and deposition of thin films and the diversity of etching chemistries developed for silicon wafer processing (referred to collectively as the Microelectricalmechanical systems (MEMS) toolkit) in several innovative ways to generate slits and pores in thin membranes. Fissell et Al. grew sacrificial oxide layers over the tops and sides of long rectangular trenches, filled in the trenches, and finished by etching through the vertical oxide layer, leaving long thin slits of excellent uniformity and tunable width [47]. A similar process was used by Desai et. Al. to manufacture circular pores [48]. The membranes are limited in their hydraulic permeabilities because of the thickness of the membrane (the depth of the slits), which are on the order of tens of microns. Their length also renders them more prone to fouling, necessitating chemical functionalization of their surfaces [33].

2.5 Block Copolymer

Block copolymers exploit the maturity of polymer chemistry technology to covalently connect two or more chains of repeating polymers with different hydrophobicities or other properties. When mixed together in solvent at concentrations above the critical micelle concentration, the hydrophobic regions of these chains aggregate together to form uniform cylindrical or spherical micelles, whose shape and size can be tuned by adjusting the length and relative hydrophobicity of the polymer components, as well as by adjusting concentration and solvent properties. Spin-coated onto a sacrificial scaffold (and, if the micelles are cylindrical, treated to align the cylinders perpendicularly to the surface), the insoluble core of the micelles can be etched away to reveal a freestanding polymeric membrane [30]. Such polymeric membranes have been used for virus separations [49], separation of macromolecules [50, 51], and long-term protein release systems [52], but lack mechanical robustness. If instead the micelles are spun-coated onto SiO_2, crystalline Si, or Si_3N_4, the block copolymer film can be used as a pore transfer template [53], and using standard photolithography and etching techniques results in a nanoporous silicon membrane that can be used for macromolecule separations [50, 54]. Pore distributions are highly tunable both through block copolymer chemistry adjustments and through the etching process, and are generally very uniform with high porosities.

2.6 Direct Drilling

In this class of methods, individual holes are drilled into a substrate using a variety of techniques, including focused ion beam drilling, e-beam lithograph [55], or e-beam drilling in a TEM [56]. For example, Tong et. Al. were able to use a focused ion beam to directly drill through a 10 nm thick silicon nitride film to produce an array of 25 nm cylindrical pores [57]. Although Prabhu et. Al. were able to separate 22 and 58 nm polystyrene

particles using a single focused ion beam-drilled pore [58], and though pore uniformity is excellent, porosity can be arbitrarily determined, and the membranes can be made quite thin, the infeasibility of drilling more than a few dozen holes at a time makes these membranes unlikely to see widespread use in filtration. The potential to use these membranes for DNA sequencing [38], however, means that the technology will continue to receive a great deal of attention and optimization.

3 Applications:

3.1 Hemodialysis

The kidney functions as a biological ultrafilter and removes excess liquid, urea, creatinine, and other metabolic products from the blood, while retaining salt and other necessary nutrients. Loss of kidney function was universally fatal until Kolf et Al invented the rotating drum dialyzer in 1945, which used an ultrafilter made of cellulose to purify blood [2, 59]. The first dialysers were used for temporary kidney failure, until improvements in the original design and the invention of the plastic shunt allowed the device to be used to treat chronic renal failure in the 1960's [60]. The most prevalent therapeutic treatment using artificial membranes is hemodialysis [61]. In 2012, more than 400,000 Americans were on dialysis [62], and as the population ages this number will increase at a rate of more than 8% per year [63]. The first dialysis membranes used were made of cellulose and remained so until the mid-90s [1]. Low hydraulic flux and blood compatibility issues eventually prompted a switch to synthetic polymer membranes, which perform better. Even the new synthetic membranes, however, fail to separate similarly size particles with the precision achieved by the kidney (Figure 4). In particular, middle weight proteins such as β2-microglobulin accumulate in the joints of patients on long term dialysis, leading to poorer patient mortality [64, 65, 66]. Next generation artificial kidneys will require

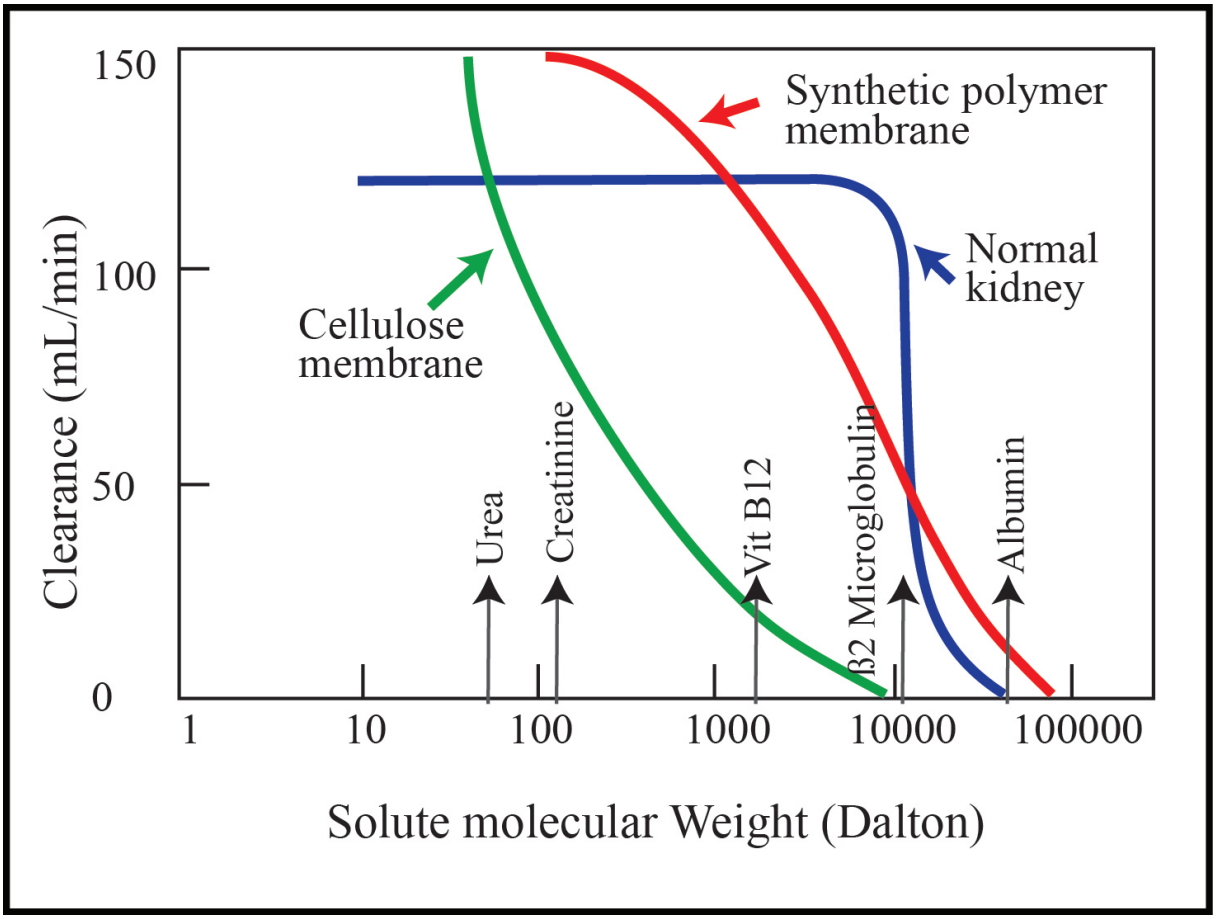

Figure 4: Typical dialysis membranes do a poor job of fractionating the components of blood. Note that the cellulose membranes pictured retain both β2-microglobulin and albumin, while the synthetic polymer membrane removes both β2-microglobulin and albumin, so that neither process is ideal. Image adapted from [1]

membranes with better cutoffs and higher water flux rates [67].

Ahmadi et. Al. showed that simple PEG coatings on pnc-Si nanomembranes can be used to reduce blood activation substantially, and were able to dialyze creatinine and smaller molecules from whole human blood samples while totally retaining hematocrit [34]. Johnson et. Al. were able to demonstrate the separation of BSA and cytochrome c (which is a size analog of the middle weight toxin β2-microglobulin) in un-PEG-lyated membrane, and used PEG-coated membranes to demonstrate reduced protein absorbtion. They were also able to dialyze urea away from a mixture of urea and fetal bovine serum using PEG-coated chips [35]. Fissell et. Al. used PEG-lyated micromachined slits to verify current electrostatic models of particle rejection [7] using a ficoll size ladder in whole cow's blood, but the membranes investigated were not able to totally retain BSA, meaning the optimized slit width is slightly thinner than the 10 nm slits they used [33].

3.2 Biotech Therapeutics Preparation

Membrane are ubiquitous in the production and purification of therapeutic biotechnology products [20], with typical biotech preparations utilizing between 10 to 20 membrane-based separations [68]. The first biotechnology product - insulin - was derived at great effort from fresh ox pancreases, where concentrations of the macromolecule was around 0.7 g/kilo of pancreas [69]. Modern processes use highly optimized transgenetic cells in large fermentation batches to produce higher initial concentrations (typically in the range of 1-3 g/L) of protein, but as yields have gotten higher therapeutics have moved beyond the highly active hormones, thrombolytic agents, and clotting factors (which act as bio-catalysts at very low concentrations) to a variety of therapeutic monoclonal antibodies, which bind stoichiometrically to a given receptor and which require much higher dosages for therapeutic effect [12]. Efficient concentration of protein is still very much an area of

interest, with typical targets on the order of micrograms of undesired host cell protein per gram of the protein of interest [20], and strict regulatory requirements governing the final concentrations of various other impurities[19]. Silicon nanomembranes capable of precisely fractionating macromolecules will likely be useful for sterile filtration, the removal of DNA, endotoxins, and viruses to concentrations below regulatory guidelines, the removal of cellular debris (especially proteolytic components that can degrade the final product), growth medium components such as growth factors and antifoaming factors, product variant removal (such as aggregates [20], deamidated, oxidized, and glycosylation forms [21]), and buffer exchange and final product concentration. Obstacles to the widespread implementation of silicon nanomembranes in industrial preparations include their propensity to irreversibly foul over time (which may be ameliorated by protein coatings such as PEG) and their higher costs relative to inexpensive reconstituted cellulose membranes.

While the potential applications of silicon nanomembranes to bioprocessing are numerous, the technology is nascent, and demonstrations of practical separations are as yet sparse. Montagne et. Al. were able to use a block-copolymer-templated nanoporous silicon nitride film to demonstrate dramatically better diffusion rates of fluorescein compared to two commercial polymeric membranes, and difference, size-dependent diffusion rates for a FITC-labelled dextran size ladder (although they were not able to totally retain even the largest dextran in the ladder) [54]. Ileri et. Al. used SiN membranes patterned with interferometric lithography to demonstrate the pH dependent transport of BSA and bovine hemoglobin. Rates of diffusion were substantially higher through their membrane than through polycarbonate track-etched membranes of a similar pore size, but the fairly large pore sizes of the membranes ($\sim$200 nm) meant few proteins could be retained by this method. Desai et. Al. used micromachined silicon/polysilicon membranes to largely

retain IgG (1% of the original concentration passed through the membrane in a day) while passing insulin and glucose [48]. Snyder et. Al. interrogated the diffusive behavior of a size ladder of proteins through pnc-Si membranes [41]. Further work indicated pnc-Si can be used to dead-end filter a protein size ladder with a well defined molecular weight cutoff [40], which Johnson et. Al. demonstrated with a dead-end separation of the smaller cytochrome *c* from BSA [35].

Another potential application of silicon nanomembranes is for the cleanup of conjugated nanoparticle-antibody preparations. Typically, quantum dots or other nanoparticles are covalently attached to monoclonal antibodies. Before this therapeutic preparation can be injected into a patient, the unconjugated antibody must be removed [70]. Figure 5 illustrates that NPN membranes can perform such a separation.

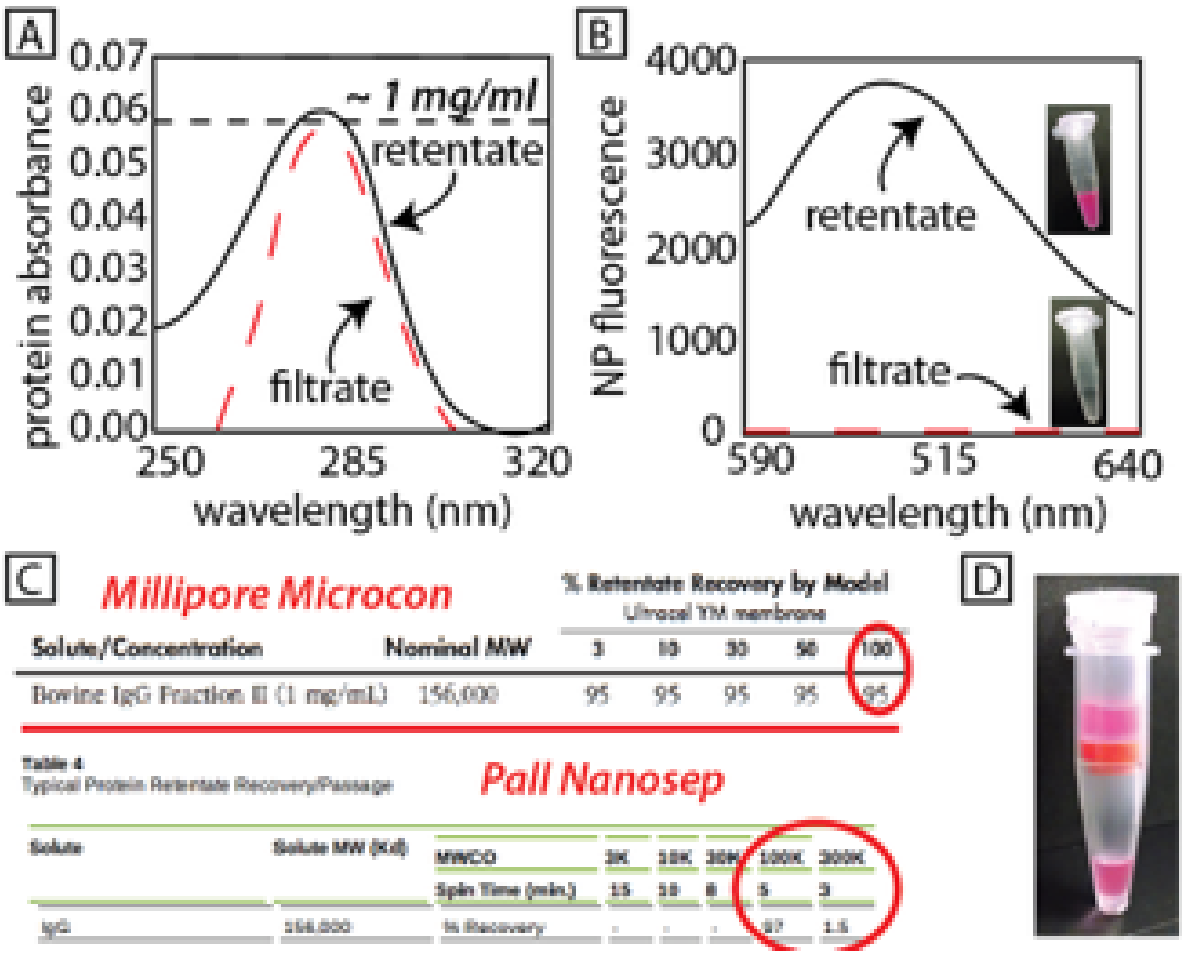

Figure 5: The unique ability of NPN nanomembranes to Separate IgG and 20 nm nanoparticles (A) Protein absorbance for retentate (what is held behind the membrane) and filtrate (what passes through the membrane) fractions as measured using a Tecan Nanoquant plate (IgG start = 1 mg/mL). Note that IgG passes through silicon nanomembrane filters with little hindrance. (B) Fluorescence nanoparticles (20 nm at 10^{15} parts/mL) in retentate and filtrate fractions. Spectra and inset images show complete retention of nanoparticles (C) Literature from Millipore and Pall indicates that only the Pall 300 kD filter should pass IgG. (D) Study with 300kD Pall Nanosep demonstrates passage of 20 nm nanoparticles

Although the capability of nanoporous membranes to differentiate between similarly size proteins has been demonstrated, clearly there is more work ahead to bring this separation technology to fruition.

References

[1] Richard Baker. *Membrane Technology and Applications (3rd Edition)*. John Wiley & Sons, Somerset, NJ, USA, 2012.

[2] W. J. Kolff, H. TH. J. Berk, Nurse M. Welle, A. J. W. van der Ley, E. C. van Dijk, and J. van Noordwijk. The artificial kidney: a dialyser with a great area. *Acta Medica Scandinavica*, 117(2):121–134, 1944.

[3] M. Bier. *Membrane Processes in Industry and Biomedicine: Proceedings of a Symposium held at the 160th National Meeting of the American Chemical Society, under the sponsorship of the Division of Industrial and Engineering Chemistry, Chicago, Illinois, September 16 and 17, 1970*. Springer US, 2012.

[4] Fresenius SE and Co KGaA. Annual report 2013. Technical report, Fresenius Medical Care AG and Co KGaA, Else-Kröner-Straße 1, Bad Homburg v. d. H., 2013.

[5] BCC Research. Ultrafiltration membranes: Technologies and the u.s. market. Technical Report MST044C, BCC Research, 2010.

[6] JD Ferry. Statistical evaluation of sieve constants in ultrafiltration. *Journal of General Physiology*, 20(1):95–104, SEP 1936.

[7] WM Deen. Hindered transport of large molecules in liquid-filled pores. *AICHE Journal*, 33(9):1409–1425, SEP 1987.

[8] FG Smith and WM Deen. Electrostatic effects on the partitioning of spherical colloids between dilute bulk solution and cylindrical pores. *Journal of Colloid and Interface Science*, 91(2):571–590, 1983.

[9] Panadda Dechadilok and William M. Deen. Electrostatic and electrokinetic effects on hindered diffusion in pores. *Journal of Membrane Science*, 336(1-2):7–16, JUL 1 2009.

[10] P. Dechadilok and W. M. Deen. Electrostatic and electrokinetic effects on hindered convection in pores. *Journal of Colloid and Interface Science*, 338(1):135–144, Oct 2009.

[11] Basavaraju Agasanapura, Ruth E. Baltus, Charan Tanneru, and Shankararaman Chellam. Membrane Rejection of Nonspherical Particles: Modeling and Experiment. *AICHE Journal*, 59(10):3863–3873, OCT 2013.

[12] S Mochizuki and AL Zydney. Theoretical analysis of pore-size distribution effects on membrane transport. *Journal of Membrane Science*, 82(3):211–227, JUL 29 1993.

[13] WS Opong and AL Zydney. Diffusive and convective protein transport through asymmetric membranes. *AICHE Journal*, 37(10):1497–1510, OCT 1991.

[14] Panadda Dechadilok and William M. Deen. Hindrance factors for diffusion and convection in pores. *Industrial and Engineering Chemistry Research*, 45(21):6953–6959, OCT 11 2006.

[15] CC Ho and AL Zydney. Transmembrane pressure profiles during constant flux. microfiltration of bovine serum albumin. *Journal of Membrane Science*, 209(2):363–377, NOV 15 2002.

[16] S Mochizuki and AL Zydney. Sieving characteristics of albumin deposits formed during microfiltration. *Journal of Colloid and Interface Science*, 158(1):136–145, JUN 1993.

[17] Chia-Chi Ho and Andrew L. Zydney. A combined pore blockage and cake filtration model for protein fouling during microfiltration. *Journal of Colloid and Interface Science*, 232(2):389 – 399, 2000.

[18] AL Zydney. Stagnant film model for concentration polarization in membrane systems. *Journal of Membrane Science*, 130(1-2):275–281, JUL 23 1997.

[19] Alan S. Michaels. Analysis and prediction of sieving curves for ultrafiltration membranes: A universal correlation? *Separation Science and Technology*, 15(6):1305–1322, 1980.

[20] Robert van Reis and Andrew Zydney. Bioprocess membrane technology. *Journal of Membrane Science*, 297(1-2):16–50, JUL 5 2007.

[21] Amit Mehta and Andrew L Zydney. Permeability and selectivity analysis for ultrafiltration membranes. *Journal of Membrane Science*, 249(1):245–249, 2005.

[22] Thomas R. Gaborski, Jessica L. Snyder, Christopher C. Striemer, David Z. Fang, Michael Hoffman, Philippe M. Fauchet, and James L. McGrath. High-Performance Separation of Nanoparticles with Ultrathin Porous Nanocrystalline Silicon Membranes. *ACS Nano*, 4(11):6973–6981, Nov 2010.

[23] Ralph Allen Sampson. On stokes's current function. *Philosophical Transactions of the Royal Society of London.(A.)*, 182:449–518, 1891.

[24] Christopher C. Striemer, Thomas R. Gaborski, James L. McGrath, and Philippe M. Fauchet. Charge- and size-based separation of macromolecules using ultrathin silicon membranes. *Nature*, 445(7129):749–753, 02 2007.

[25] AP Li, F Muller, A Birner, K Nielsch, and U Gosele. Hexagonal pore arrays with a 50-420 nm interpore distance formed by self-organization in anodic alumina. *Journal of Applied Physics*, 84(11):6023–6026, DEC 1 1998.

[26] H Masuda and K Fukuda. Ordered metal nanohole arrays made by a 2-step replication of honeycomb structures of anodic alumina. *Science*, 268(5216):1466–1468, JUN 9 1995.

[27] M Majumder, N Chopra, R Andrews, and BJ Hinds. Nanoscale hydrodynamics - Enhanced flow in carbon nanotubes. *Nature*, 438(7064):44, NOV 3 2005.

[28] JK Holt, HG Park, YM Wang, M Stadermann, AB Artyukhin, CP Grigoropoulos, A Noy, and O Bakajin. Fast mass transport through sub-2-nanometer carbon nanotubes. *Science*, 312(5776):1034–1037, MAY 19 2006.

[29] Miao Yu, Hans H. Funke, John L. Falconer, and Richard D. Noble. High Density, Vertically-Aligned Carbon Nanotube Membranes. *Nano Letters*, 9(1):225–229, JAN 2009.

[30] Elizabeth A. Jackson and Marc A. Hillmyer. Nanoporous Membranes Derived from Block Copolymers: From Drug Delivery to Water Filtration. *ACS Nano*, 4(7):3548–3553, JUL 2010.

[31] TA Desai, DJ Hansford, L Leoni, M Essenpreis, and M Ferrari. Nanoporous antifouling silicon membranes for biosensor applications. *Biosensors and Bioelectronics*, 15(9-10):453–462, NOV 2000.

[32] Lalitha Muthusubramaniam, Rachel Lowe, William H. Fissell, Lingyan Li, Roger E. Marchant, Tejal A. Desai, and Shuvo Roy. Hemocompatibility of Silicon-Based Sub-

strates for Biomedical Implant Applications. *Annals of Biomedical Engineering*, 39(4):1296–1305, APR 2011.

[33] William H. Fissell, Anna Dubnisheva, Abigail N. Eldridge, Aaron J. Fleischman, Andrew L. Zydney, and Shuvo Roy. High-performance silicon nanopore hemofiltration membranes. *Journal of Membrane Science*, 326(1):58 – 63, 2009.

[34] Morteza Ahmadi, Maud Gorbet, and John T. W. Yeow. In vitro Clearance and Hemocompatibility Assessment of Ultrathin Nanoporous Silicon Membranes for Hemodialysis Applications Using Human Whole Blood. *Blood Purification*, 35(4):305–313, 2013.

[35] Dean G. Johnson, Tejas S. Khire, Yekaterina L. Lyubarskaya, Karl J.P. Smith, Jon-Paul S. DesOrmeaux, Jeremy G. Taylor, Thomas R. Gaborski, Alexander A. Shestopalov, Christopher C. Striemer, and James L. McGrath. Ultrathin silicon membranes for wearable dialysis. *Advances in Chronic Kidney Disease*, 20(6):508 – 515, 2013. Nanotechnology and the Kidney.

[36] S Sharma, RW Johnson, and TA Desai. Evaluation of the stability of nonfouling ultrathin poly(ethylene glycol) films for silicon-based microdevices. *LANGMUIR*, 20(2):348–356, JAN 20 2004.

[37] William H. Fissell, Aaron J. Fleischman, H. David Humes, and Shuvo Roy. Development of continuous implantable renal replacement: past and future. *Translational Research*, 150(6):327–336, DEC 2007. 9th International Conference on Dialysis, Austin, TX, JAN 24-26, 2007.

[38] Ken Healy, Birgitta Schiedt, and Alan P Morrison. Solid-state nanopore technologies for nanopore-based dna analysis. *Nanomedicine*, 2(6):875–897, 2014/10/06 2007.

[39] Ivan Vlassiouk, Pavel Y. Apel, Sergey N. Dmitriev, Ken Healy, and Zuzanna S. Siwy. Versatile ultrathin nanoporous silicon nitride membranes. *Proceedings of the National Academy of Sciences of the United States of America*, 106(50):21039–21044, DEC 15 2009.

[40] J.L. Snyder. *Porous Nanocrystalline Silicon Membranes as Sieves and Pumps*. PhD thesis, University of Rochester, 2011.

[41] J.L. Snyder, A. Clark Jr., D.Z. Fang, T.R. Gaborski, C.C. Striemer, P.M. Fauchet, and J.L. McGrath. An experimental and theoretical analysis of molecular separations by diffusion through ultrathin nanoporous membranes. *Journal of Membrane Science*, 369(1–2):119 – 129, 2011.

[42] J P S DesOrmeaux, J D Winans, S E Wayson, T R Gaborski, T S Khire, C C Striemer, and J L McGrath. Nanoporous silicon nitride membranes fabricated from porous nanocrystalline silicon templates. *Nanoscale*, 6(18):10798–10805, Sep 2014.

[43] Nazar Ileri, Roland Faller, Ahmet Palazoglu, Sonia E. Letant, Joseph W. Tringe, and Pieter Stroeve. Molecular transport of proteins through nanoporous membranes fabricated by interferometric lithography. *Phys. Chem. Chem. Phys.*, 15:965–971, 2013.

[44] W.M. Zhang, J. Li, L.X. Cao, Y.G. Wang, W. Guo, K.X. Liu, and J.M. Xue. Fabrication of nanoporous silicon dioxide/silicon nitride membranes using etched ion track technique. *Nuclear Instruments and Methods in Physics Research Section B: Beam Interactions with Materials and Atoms*, 266(12–13):3166 – 3169, 2008. Radiation Effects in Insulators Proceedings of the Fourteenth International Conference

on Radiation Effects in Insulators Fourteenth International Conference on Radiation Effects in Insulators.

[45] S Kuiper, CJM van Rijn, W Nijdam, and MC Elwenspoek. Development and applications of very high flux microfiltration membranes. *Journal of Membrane Science*, 150(1):1–8, NOV 11 1998.

[46] Nazar Ileri, Pieter Stroeve, Ahmet Palazoglu, Roland Faller, Saleem H. Zaidi, Hoang T. Nguyen, Jerald A. Britten, Sonia E. Letant, and Joseph W. Tringe. Fabrication of functional silicon-based nanoporous membranes. *Journal of Micro-Nanolithography MEMS and MOEMS*, 11(1), JAN-MAR 2012.

[47] William H. Fissell, Sargum Manley, Anna Dubnisheva, Jeffrey Glass, Jeffrey Magistrelli, Abigail N. Eldridge, Aaron J. Fleischman, Andrew L. Zydney, and Shuvo Roy. Ficoll is not a rigid sphere. *American Journal of Physiology - Renal Physiology*, 2007.

[48] Tejal A Desai, Derek Hansford, and Mauro Ferrari. Characterization of micromachined silicon membranes for immunoisolation and bioseparation applications. *Journal of Membrane Science*, 159(1–2):221 – 231, 1999.

[49] Seung Yun Yang, Jihoon Park, Jinhwan Yoon, Moonhor Ree, Sung Key Jang, and Jin Kon Kim. Virus filtration membranes prepared from nanoporous block copolymers with good dimensional stability under high pressures and excellent solvent resistance. *Advanced Functional Materials*, 18(9):1371–1377, MAY 9 2008.

[50] Eric E. Nuxoll, Marc A. Hillmyer, Ruifang Wang, C. Leighton, and Ronald A. Siegel. Composite Block Polymer-Microfabricated Silicon Nanoporous Membrane. *ACS Applied Materials and Interfaces*, 1(4):888–893, APR 2009.

[51] Hiroki Uehara, Masaki Kakiage, Miho Sekiya, Daisuke Sakuma, Takeshi Yamonobe, Nao Takano, Antoine Barraud, Eric Meurville, and Peter Ryser. Size-Selective Diffusion in Nanoporous but Flexible Membranes for Glucose Sensors. *ACS Nano*, 3(4):924–932, APR 2009.

[52] Seung Yun Yang, Jeong-A Yang, Eung-Sam Kim, Gumhye Jeon, Eun Ju Oh, Kwan Yong Choi, Sei Kwang Hahn, and Jin Kon Kim. Single-File Diffusion of Protein Drugs through Cylindrical Nanochannels. *ACS Nano*, 4(7):3817–3822, JUL 2010.

[53] Ana-Maria Popa, Philippe Niedermann, Harry Heinzelmann, Jeffrey A Hubbell, and Raphaël Pugin. Fabrication of nanopore arrays and ultrathin silicon nitride membranes by block-copolymer-assisted lithography. *Nanotechnology*, 20(48):485303, 2009.

[54] Franck Montagne, Nicolas Blondiaux, Alexandre Bojko, and Raphael Pugin. Molecular transport through nanoporous silicon nitride membranes produced from self-assembling block copolymers. *Nanoscale*, 4:5880–5886, 2012.

[55] A. J. Storm, J. H. Chen, X. S. Ling, H. W. Zandbergen, and C. Dekker. Fabrication of solid-state nanopores with single-nanometre precision. *Nat Mater*, 2(8):537–540, 08 2003.

[56] Meng-Yue Wu, Diego Krapf, Mathijs Zandbergen, Henny Zandbergen, and Philip E. Batson. Formation of nanopores in a sinsio2 membrane with an electron beam. *Applied Physics Letters*, 87(11):–, 2005.

[57] HD Tong, HV Jansen, VJ Gadgil, CG Bostan, E Berenschot, CJM van Rijn, and M Elwenspoek. Silicon nitride nanosieve membrane. *Nano Letters*, 4(2):283–287, FEB 2004.

[58] Anmiv S. Prabhu, Talukder Zaki N. Jubery, Kevin J. Freedman, Rafael Mulero, Prashanta Dutta, and Min Jun Kim. Chemically modified solid state nanopores for high throughput nanoparticle separation. *Journal of Physics - Condensed Matter*, 22(45), NOV 17 2010.

[59] Willem J Kolff, J Van Noordwijk, and NKM de Leeuw. *New Ways of Treating Uraemia: The Artificial Kidney Peritoneal Lavage, Intestinal Lavage*. Churchill, 1947.

[60] Wayne Quinton, David Dillard, and Belding H Scribner. Cannulation of blood vessels for prolonged hemodialysis. *ASAIO Journal*, 6(1):104–113, 1960.

[61] Aileen Grassmann, Simona Gioberge, Stefan Moeller, and Gail Brown. Esrd patients in 2004: global overview of patient numbers, treatment modalities and associated trends. *Nephrology Dialysis Transplantation*, 20(12):2587–2593, 2005.

[62] U.S. Renal Data System. Usrds 2014 annual data report: Atlas of end-stage renal disease in the united states. Technical report, National Institute of Diabetes and Digestive and Kidney Diseases,, Bethesda, MD, 2014.

[63] Arrigo Schieppati and Giuseppe Remuzzi. Chronic renal diseases as a public health problem: epidemiology, social, and economic implications. *Kidney Int Suppl*, pages S7–S10, Sep 2005.

[64] R Vanholder, R De Smet, G Glorieux, A Argiles, U Baurmeister, P Brunet, W Clark, G Cohen, PP De Deyn, R Deppisch, B Descamps-Latscha, T Henle, A Jorres,

HD Lemke, ZA Massy, J Passlick-Deetjen, M Rodriguez, B Stegmayr, P Stenvinkel, C Tetta, C Wanner, W Zidek, and EUTox Grp. Review on uremic toxins: Classification, concentration, and interindividual variability. *Kidney International*, 63(5):1934–1943, MAY 2003.

[65] M Jadoul. Dialysis-related amyloidosis: importance of biocompatibility and age. *Nephrology Dialysis Transplantation*, 13(7):61–64, 1998. 1st Symposium on Renal Disease and Ageing, Modena, Italy, SEP 15-16, 1995.

[66] Alfred K. Cheung, Michael V. Rocco, Guofen Yan, John K. Leypoldt, Nathan W. Levin, Tom Greene, Lawrence Agodoa, James Bailey, Gerald J. Beck, William Clark, Andrew S. Levey, Daniel B. Ornt, Gerald Schulman, Steven Schwab, Brendan Teehan, Garabed Eknoyan, and HEMO Study Grp. Serum beta-2 microglobulin levels predict mortality in dialysis patients: Results of the HEMO study. *Journal of the American Society of Nephrology*, 17(2):546–555, FEB 2006.

[67] H David Humes, Deborah Buffington, Angela J Westover, Shuvo Roy, and William H Fissell. The bioartificial kidney: current status and future promise. *Pediatr Nephrol*, 29(3):343–351, Mar 2014.

[68] A. S. Rathore and A. Shirke. Recent developments in membrane-based separations in biotechnology processes: review. *Preparative Biochemistry and Biotechnology*, 41(4):398–421, 2011. PMID: 21967339.

[69] Harold Ward Dudley. The purification of insulin and some of its properties. *Biochemical Journal*, 17(3):376–390, 1923.

[70] Mark Howarth, Wenhao Liu, Sujiet Puthenveetil, Yi Zheng, Lisa F. Marshall, Michael M. Schmidt, K. Dane Wittrup, Moungi G. Bawendi, and Alice Y. Ting.

Monovalent, reduced-size quantum dots for imaging receptors on living cells. *Nature Methods*, 5(5):397–399, MAY 2008.